Biointerface Research in Applied Chemistry
Platinum Open Access Journal (ISSN: 2069-5837)

Article
Volume 11, Issue 2, 2021, 9062 - 9070
https://doi.org/10.33263/BRIAC112.90629070

X-Ray Diffraction and Magnetic Properties of Nd Substituted $NiZnFe_2O_4$ Characterized by Rietveld Refinement

Kokkanda Ratnaih [1], Venkata Krishna Prasad N [1,*], Ramesh Singampalli [1], M.S.S.R.K.N.Sarma [1], G.S.V.R.K.Choudary [2], Srinivasa Rao Kurapati [3]

[1] Department of Physics, School of Science, GITAM University, Bengaluru, India
[2] Department of Physics, Bhavan's Vivekananda College, Sainikpuri, Secunderabad, India
[3] Department of Physics, PBN College, Nidubrolu, India
* Correspondence: drnvkprasad@gmail.com;

Scopus Author ID 8356816900
Received: 8.07.2020; Revised: 27.08.2020; Accepted: 28.08.2020; Published: 1.09.2020

Abstract: Solid-state method developed neodymium-doped Ni-Zn ferrites exhibit additional orthoferrite and α-Fe_2O_3 phases. The change in magnetic properties and lattice parameters are influenced by above mentioned extra phases other than the Nickel-Zinc ferrite spinel structure. Observations indicate that curie temperature, as well as saturation magnetization, reduce with an increase in Neodymium concentration. At the same time, for Nd = 0.02, initial permeability has been slightly increased. This paper explains the reason for these changes in terms of diluted octahedral sites replaced with Nd ions instead of Fe-ions and the number of additional phases that are present.

Keywords: Ferrites; Orthoferrites; Magnetization; Lattice constant; Neodymium; Zinc.

1. Introduction

Soft magnetic materials exhibiting nanosized dimensions are of prime significance today in the research perspective as a result of their dielectric, electric, and magnetic properties. Nickel-Zinc ferrites exhibit high electrical resistivity, curie temperature, and low current loss. These ferrites are significant and versatile materials with various applications in transformer cores, radiofrequency devices, microwave absorbers, wave absorbers, inductors, magnetic recording media, and power transformers, etc. [1-6]. They exhibit electrical resistivity of high value in the range of 10^5 to 10^8 ohm-cm with moderate permeability and magnetization, eddy current losses of low value because of more electrical resistivity making them suitable for high-frequency applications [7-8]. Rare earth is being doped to increase further permeability and magnetization as rare-earth ions have a high magnetic moment. At the same time, rare earth ion induction might lead to lattice distortion, internal stress may be generated due to causing of heterogeneity in structure. A critical investigation is required to study the structure of spinel lattice in terms of their site occupancy [9-10].

It is already reported that rare-earth ions having low ionic radii come into spinel lattice while ions of large radii get diffused into grain boundaries, which form an extremely thin layer around these grains. The above changes drastically alter ferrites properties demanding demands thorough examination of the system. Therefore it is definitely necessary to study the effect of

added neodymium on-site occupancy as well as segregation related to the Nickel-Zinc ferrite system [11-13].

This paper gives an elaborate explanation regarding structural properties as well as magnetic properties of Ni-Zn ferrites substituted with neodymium having basic composition $Ni_{0.65}Zn_{0.35}Fe_2O_4$. Many methods for the preparation of samples to fabricate nanomaterials are available, which include micro-emulsion [14], co-precipitation [15], sol-gel [16], co-precipitation [17], citrate precursor, ceramic sintering, refluxing [18], and solid-state chemical reaction [19] methods. In the present work, we adopted a solid-state reaction method for the preparation of ferrite mentioned above. Explanation of variation observed in saturation magnetization, coercivity, and lattice constant was done on the basis of orthoferrite additional phases and iron oxide present in the samples.

2. Materials and Methods

By using the regular ceramic method, a series of samples with composition $Ni_{0.65}Zn_{0.35}Nd_xFe_{2-x}O_4$ where x = 0.00 to 0.10 in steps of 0.02 were prepared. Fe_2O_3 (98.5%), NiO (99.9%), ZnO (99.5%), and Nd_2O_3 (99.9%) of high purity analytical grade were considered with a nonstoichiometric ratio for maintaining excess iron oxide of ten to fifteen percent and finely crushed. After crushing, they were thoroughly mixed and ground in acetone media for 4 hours by using agate mortar and pestle. Calcination of this mixed homogeneous powder was done at a temperature of 900°C in the air for 2 hours and then is made to undergo slow cooling. Uniformly sized crystallites of small size were prepared from this powder in pre-sintered condition by crushing another time and grinding thoroughly for two hours in acetone medium. Pellets and toroids were made from the mixer with the help of a binder (fifteen percent polyvinyl alcohol) having 3 tons/inch^2 and 5 tons/inch^2 a uniaxial pressure of essentially.

Pellets were of thickness 4 mm and diameter of 3 mm while toroids of inner diameter 13 mm and outer diameter 18 mm were prepared. These toroids and pellets are lastly sintered at a temperature of 1250°C in the air for 2 hours period and cooled in a natural way. Polishing of sample surfaces was done in order to remove the oxide layer formed, if any, while sintering process.

3. Results and Discussion

3.1. Structural analysis.

3.1.1. X-ray diffraction and Rietveld refinement.

X-ray diffraction studies confirm the spinel structure. The lattice parameter values acquired for every reflected plane were plotted against the Nelson-Riley function [20, 21].

$$F(\theta) = (1/2)[\cos^2\theta/\sin\theta + \cos^2\theta/\theta].$$

Estimation of accurate or nearest a_0 (lattice constant) value for each individual sample has been done by extrapolating these lines $F(\theta) = 0$. X-ray diffraction patterns indicate that measurements of lattice constant (a = 8.3840 A°) correlate with that of the reported [22-24]. Figure 1a shows additional lines in all samples with neodymium, whose intensity increases with an increase in impurity concentration. These additional lines are assumed to be those which correspond to $NdFeO_3$ second phase [25, 26]. Diffraction patterns of the sample for x = 0.02, 0.04, 0.06, 0.08, and 0.10 were shown in Fig.1 while Table 1. lists their structural

properties. Rietveld analysis is shown in Figures 1b and 1c, which indicate GOF for all samples and are given in Table.1. Extra peaks related to α-Fe_2O_3 are due to the presence of iron oxide that was inducted into the ferrite system as a stoichiometric conscious of providing accommodation for Neodymium ions of high radii, high concentration, which was found to be incapable of producing [27, 28]. Figures 2a and 2b represent Rietveld refined XRD spectra, while Table 1. shows the phase contents and lattice parameters.

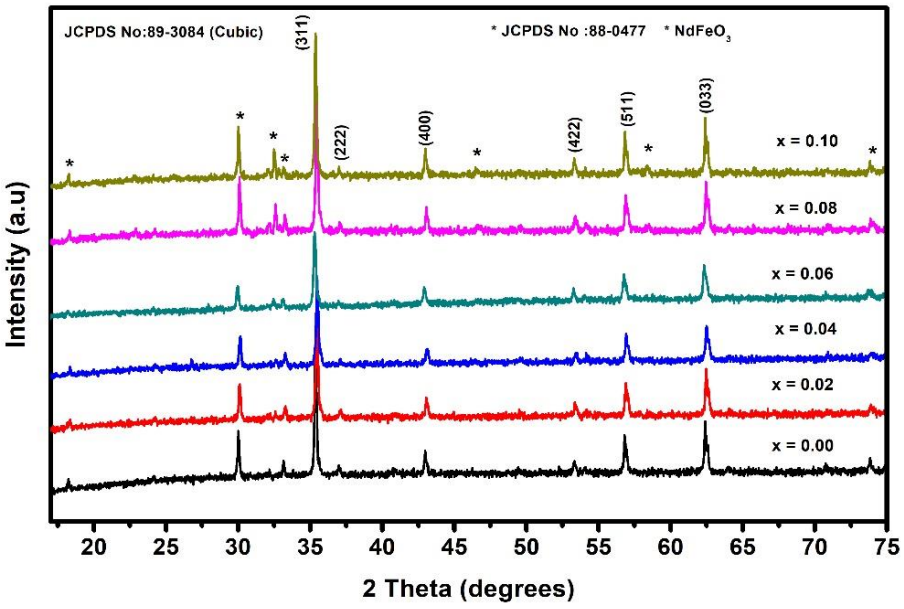

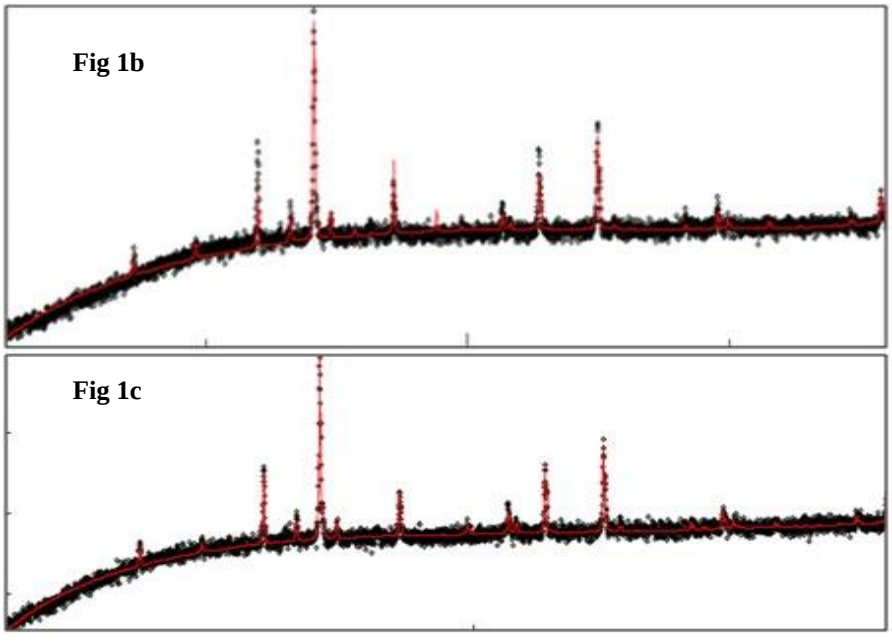

Figure 1a. X-ray Diffraction Patterns of $Ni_{0.65}Zn_{0.35}Nd_xFe_{2-x}O_4$; 1b.Rietveld refined XRD of Nickel - ZincFerrite; 1c. Rietveld refined XRD of Neodymium doped Nickel-ZincFerrite for x=0.02

3.1.2. Magnetic properties.

Hysteresis curves for the developed sample ($Ni_{0.65}Zn_{0.35}Fe_{2-x}Nd_xO_4$ where x= 0.02 to 0.10 with steps of 0.02) are shown in Figure 2 while their magnetic properties like Remanence, Coercivity, and Saturation Magnetization ((M_r, H_c and M_s) are shown in Fig.3. Rare-earth

doping may dilute magnetic properties, which might disturb the Fe^{3+}-Fe^{2+} along with the interaction of 3d-4f [29-32]. The saturation magnetization (Ms) of the Ni-Zn ferrite for the substituted Nd decreases for all the compositions, but for the compositions, x = 0.06 and 0.1 observed with maximum M_s values. As a result, there an increase in Hc values, which is shown in Fig.3. The factors which are responsible for the increase of Hc are magnetocrystalline anisotropy, loss of metal cations, Bohr magneton, magnetic domain, and superexchange. Further, the increase of Hc is assumed to be due to Nd^{3+} with a more ionic radius of 0.983 Å on comparison with Fe^{3+} ion of radius 0.654 Å leading to lattice expansion as well as an increase in interplanar spacing, reducing the response of the particles to the applied magnetic field [33-38]. Improvement of Remanence (M_r) from x = 0.04 indicate exchange interactions moderation [39, 40] .

Table 1.XRD Analysis of Nd-doped Ni-Zn-Ferrite.

Nd content (x)	Phases present	rwp %	vol %	wt %	cell par. (Å) a	cell par. (Å) b	cell par. (Å) c	Crystallite size (Å)	microstrain
0.00	Ni-Zn		86.5503	85.7113	8.4135			2082.7666	1.7356E-5
	Iron(III) Oxide		13.4497	14.2887	5.4292	55.2840		1023.3861	1.4001E-4
0.02	Ni-ZnNd1	4.0001	82.0003	82.1459	8.4158			2260.5823	1.4098E-4
	Iron(III) Oxide		17.9997	17.8541	5.4284	55.3054		1000.1209	9.2617E-6
0.04	Ni-ZnNd2	4.7134	75.5638	75.1479	8.4164			2026.8478	1.0519E-4
	NdFeO3		3.0863	3.9968	5.5887	7.7619	5.4489	1000.0000	6.0E-4
	Iron(III) Oxide		21.3500	20.8552	5.4305	55.2930		1016.3486	3.2412E-6
0.06	Ni-ZnNd3	4.2992	80.2392	79.5580	8.4147			2283.1885	5.411E-4
	NdFeO3		4.2092	5.3917	5.5887	7.7619	5.4489	1000.0000	6.0E-4
	Iron(III) Oxide		15.5516	15.0503	5.4267	55.3113		1538.2815	3.2504E-4
0.08	Ni-ZnNd8	4.1675	74.5909	73.4001	8.4155			1983.9523	7.479E-6
	NdFeO3		7.6932	9.7122	5.5887	7.7619	5.4489	1000.0000	6.0E-4
	Iron(III) Oxide		17.7159	16.8877	5.4278	55.3093		1000.0172	3.1609E-4
0.10	Ni-ZnNd10	4.1421	80.4200	78.8452	8.4119			3168.2114	4.2091E-6
	NdFeO3		8.8989	11.0875	5.5845	7.7700	5.4525	1000.0000	6.0E-4
	Iron(III) Oxide		10.6810	10.0673	5.4274	55.2844		1020.8768	3.7252E-4

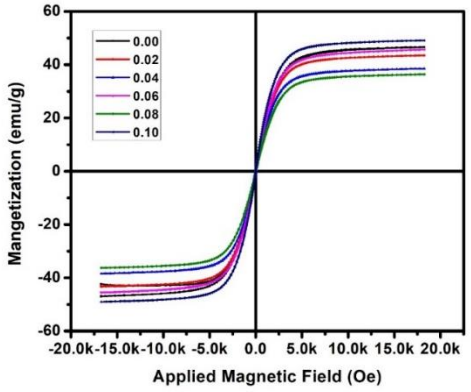

Figure 2. Hysteresis Loops of Nd^{3+} doped Nickel-Zinc Ferrite samples.

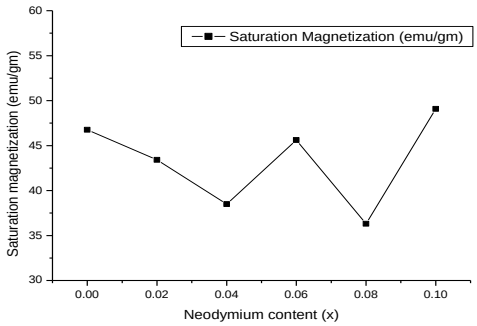

Figure 3. Saturation magnetization versus Nd^{3+} concentration in Nickel-Zinc Ferrites.

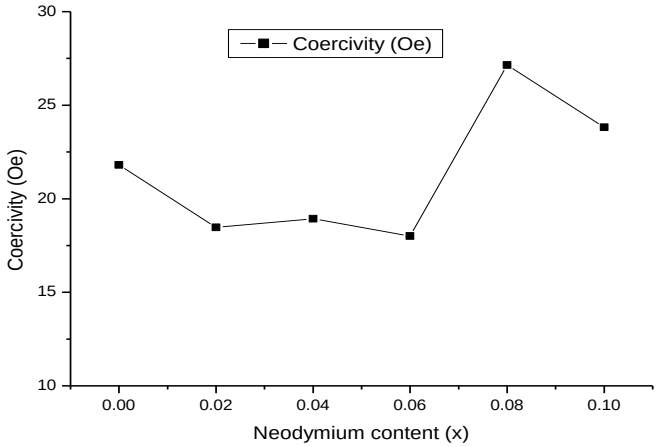

Figure 4. Coercivity variation versus Nd^{3+} concentration in Nickel-Zinc Ferrites.

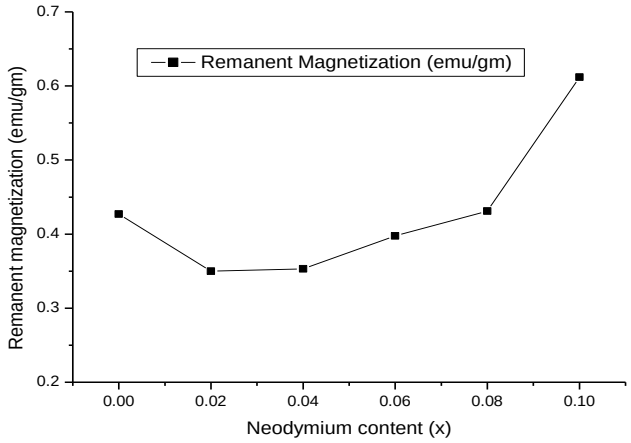

Figure 5. Remanent Magnetization versus Nd^{3+} concentration in Nickel-Zinc Ferrites.

Nd alters the magnetic moment as well as change the cubic structure based on the extent of doping[41]. Reports indicate that some of the neodymium reside at grain boundaries while others do not enter into the ferrite lattice. Also, the presence of the α-Fe_2O_3 or $REFeO_3$ phase might increase at grain boundaries at low concentration or high concentration of rare-earth-doped samples, causing some variation in magnetic properties. As evidence indicate, such a phase in present samples under investigation, magnetic properties, and their dilution may be due to several effects, as mentioned in the previous section. Samples under investigation show $NdFeO_3$ phase for concentration x = 0.040 an improved remanence or the lowest state of Ms amongst the existing samples. The initial decrease in saturation magnetization, as shown in Figure 3, is because of octahedral site dilution by Nd^{3+} ions, while its rise is due to an increase of Nd might be due to additional content of iron that enters spinel lattice. The variation of coercivity exhibited in Figure 4 and remanent magnetization are shown in Figure 5 due to the rise in neodymium content may be attributed to the reasons mentioned above [42].

3.1.3. Curie temperature.

The change in permeability with temperature for samples under investigation is shown in Figure.6. As shown in the figure, maximum permeability is found for x=0.02, while the rest

of the samples under investigation show versatile behavior. A shift towards lower temperature side is observed for Curie temperature indicate ion dilution in exchange interaction between Fe^{3+}-O-Fe^{3+} of ferrite lattice due to the presence of additional phases that include α-phase Fe_2O_3 or $NdFeO_3$ phase as indicated by diffraction studies [43]. Investigating samples are stable up to the point of curie temperature point, which indicates spinel structure deformation instead of impurity presence.

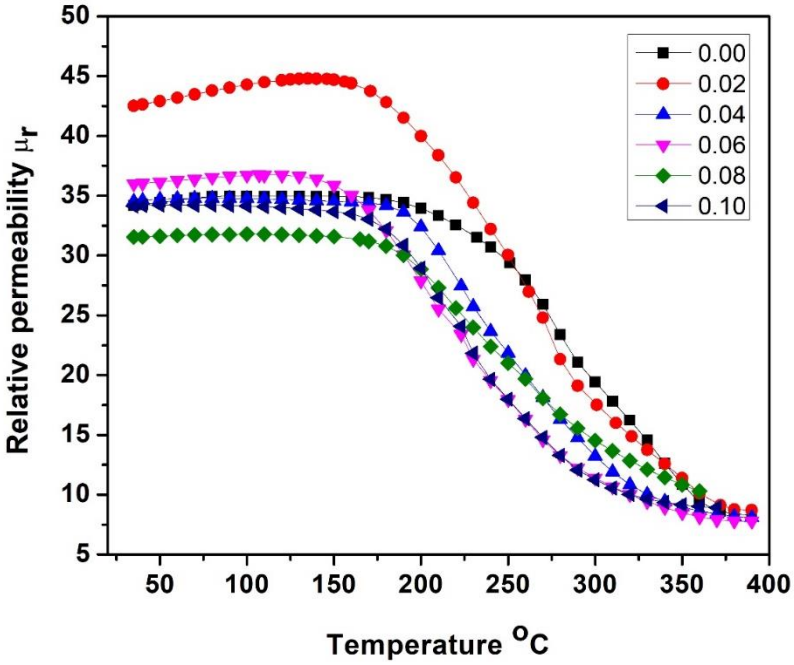

Figure 6. Relative permeability versus temperature of Nd^{3+} doped Nickel-Zinc Ferrite samples.

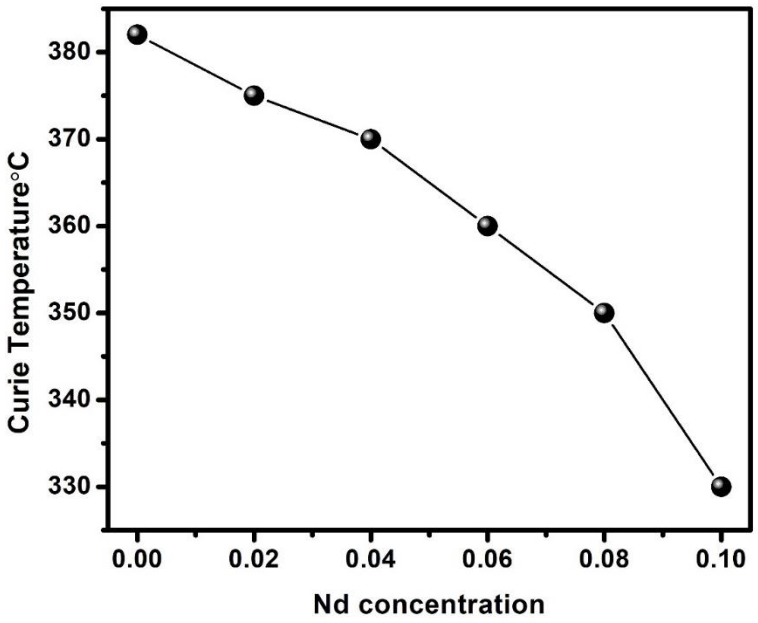

Figure 7. Variation of Curie temperature with Nd concentration.

Fig.7 indicates a decrease in Curie temperature with an increase of Nd^{3+} concentration. This can be attributed to the decrease in exchange interactions under the influence of reduced magnetic moment at B-sites as well as the presence of α-Fe_2O_3 and anti-ferromagnetic orthoferrite phases. A decrease in magnetic interaction between ferrite grains by additional phases leads to a reduction in exchange interaction [44].

4. Conclusions

Synthesis of $Ni_{0.65}Zn_{0.35}Fe_{2-x}Nd_xO_4$ for x = 0.020, 0.040, 0.060, 0.08 and 0.1 samples were done with traditional solid-state reaction method. Observed X-ray diffraction patterns indicate $NdFeO_3$ and α-Fe_2O_3 phases and their associated secondary phases along with the formation of cubic spinel phases. Rietveld refinement analysis of $Ni_{0.65}Zn_{0.35}Fe_{2-x}Nd_xO_4$ indicates primary and secondary phases. M-H curves for x = 0.10 reveal highest value of saturation magnetization equal to 49.1 emu/g while for x = 0.02 composition maximum magnetic permeability of value 42.5 was obtained. Plots related to magnetic permeability versus temperature for $Ni_{0.65}Zn_{0.35}Fe_{2-x}Nd_xO_4$ samples indicate a decrease of magnetic curie transition temperature from 382 ^oC to 330^oC as Nd content varies with x values ranging between 0.00 - 0.10 in steps of 0.02. Finally, it may be inferred that substituting neodymium leads to a decrease in magnetic exchange interactions decrease between tetrahedral (A) and octahedral (B) sites.

Funding

This research received no external funding.

Acknowledgments

The authors are grateful to the Management of GITAM (Deemed to be University), Bangaluru Campus, and Visakhapatnam campus, India.

Conflicts of Interest

The authors declare no conflict of interest.

References

1. R. Kesavamoorthi, C.R. Raja, Substitution effects on rare-earth ions doped nickel zinc ferrite nanoparticles, *J. Supercond. Nov. Magnetism* **2017**, 30, 1207–1212, https://doi.org/10.1007/s10948-016-3904-5.
2. G.S. Luo,W.P. Zhou,J.D.Li, Z.Y. Zhou,G.W. Jiang,W.S. Li, S.L. Tang,Y.W.Du, The influence of Nd^{3+} ions doping on the structural, dielectric and magnetic properties of Ni-Zn ferrites, *J. Mater. Sci. Mater. Electron.* **2017,** 28, 7259–7263, https://doi.org/10.1007/s10854-017-6408-6.
3. X. Wu, W. Chen, W. Wu, J. Wu, Q. Wang, Improvement of the magnetic moment of NiZn ferrites induced by substitution of Nd^{3+} ions for Fe^{3+} ions, *J. Magn. Magn Mater*. **2018**, 453,246–253, https:/doi.org/10.1016/j.jmmm.2018.01.057.
4. T.J. Shinde, A.B. Gadkari, P.N. Vasambekar, Structural and dielectric properties of nanocrystalline Nd^{3+} substituted nickel-zinc ferrites, *J. Mater. Sci. Mater. Electron*. **2012**, 23, 697–705, https://doi.org/10.1007/s10854-011-0474-y
5. Hamid, E.; Hamid,M. Synthesis and characterization of copper ferrite nanoparticles and its application as MRI contrast agent, *Lett. Appl.* NanoBioScience. 2019, 8 (1), 541–544. https://doi.org/10.33263/LIANBS81.541544
6. Kurtulus, G. Comparison of the effect of magnetite (Fe_3O_4) iron oxide nanoparticles on melanoma cells and healthy cells: an in vitro study, *Lett. Appl.* NanoBioScience 2020, 9(2), 1049 – 1057. https://doi.org/10.33263/LIANBS92.10491057
7. Zhang, M., Gao, X., Zi, Z., Dai, J., Wang, J., Chou, S., Liang, C., Zhu, X., Sun, Y. & Liu, H. Porous $Ni_{0.5}Zn_{0.5}Fe_2O_4$ nanospheres: synthesis, characterization, and application for lithium storage. *Electrochimica Acta* **2014**,147, 143-150, http://dx.doi.org/10.1016/j.electacta.2014.09.072.
8. G.PozoLópez,S.P.Silvetti,S.E.Urreta,A.C.Carreras, structure and magnetic properties of NiZn ferrite/SiO_2 nanocomposites synthesized by ball milling, *J. Alloy.Comp*. **2010**,505,808–813, https://doi.org/10.1016/j.jallcom.2010.06.145.
9. G. V. Bazuev, O. I. Gyrdasova, S. I. Novikov & A. Yu. Kuznetsov, Synthesis, structure, and magnetic properties of rare-earth-doped $Ni_{0.75}Zn_{0.25}Fe_2O_4$ nickel zinc ferrite, *Inorg. Mater*. **2016**, 52, 932–938, https://doi.org/10.1134/S0020168516090028.

10. R. Hochschild, H. Fuess, Rare-earth doping of nickel zinc ferrites, *J. Mater. Chem*. **2000**, 10, 539–542, https://doi.org/10.1039/A905583E.
11. S.E.Jacobo,P.G.Bercoff, Structural and electromagnetic properties of yttrium-substituted Ni–Zn ferrites, *Ceramic.Inernational*. **2016,** 42, 7664–7668, https://doi.org/10.1016/j.ceramint.2016.01.180.
12. A.Ghasemi,M.Mousavinia ,Structural and magnetic evaluation of substituted $NiZnFe_2O_4$ particles synthesized by conventional sol–gel method. *Ceramics International* **2014**, 40, 2825-2834,https://doi: 10.1016/j.ceramint.2013.10.031.
13. S.Ramesh,B.Dhanalakshmi, B.Chandra Sekhar, P.S.V.Subba Rao, B.Parvatheeswaara Rao, Effect of Mn/Co substitutions on the resistivity and dielectric properteis of nickel-zinc ferrites, Ceramic *International* **2016**, 42 , 9591-9598, https://doi.org/10.1016/j.ceramint.2016.03.043.
14. Darko Makovec,Aljosa Kosak,Andrej Žnidaršič,Miha Drofenik, The synthesis of spinel–ferrite nanoparticles using precipitation in microemulsions for ferro fluid applications, *J. Magn.Magn Mater*. ***2005***, 289, 32–35, https://doi.org/10.1016/j.jmmm.2004.11.010.
15. P.Yaseneva, M.Bowker, G.Hutchings, Structural and magnetic properties of Zn-substituted cobalt ferrites prepared by co-precipitation method, *Phys. Chem. Chem. Phys*. **2011**, 13, 18609–18614, https://doi.org/10.1039/C1CP21516G.
16. K.HuiWu, Y.ChiungChang, G.Pying Wang, Preparation of NiZn ferrite/SiO_2 nanocomposite powders by sol–gel auto-combustion method, *Journal of Magnetism and Magnetic Materials* 2004,269,150-155. https://doi.org/10.1016/S0304-8853(03)00585-7.
17. A.I.Nandapure,S.B.Kondawar,P.S.Sawadh,B.I.Nandapure, effect of zinc substitution on magnetic and electrical properties of nanocrystalline nickel ferrite synthesized by refluxing method, *Phys.B Condens.Matter* **2012**,407, 1104–1107, https://doi.org/10.1016/j.physb.2012.01.081
18. K.K.Bharathi,G.Markandeyulu,C.V.Ramana,Structural, magnetic, electrical, and magnetoelectric properties of Sm-and Ho-substituted nickel ferrites, *J.Phys.Chem* **2011**,C115554–560, https://doi.org/10.1021/jp1060864.
19. J B Nelson and D P Riley, An experimental investigation of extrapolation methods in the derivation of accurate unit-cell dimensions of crystals, *Proc. Phys. Soc* **1945**, 57, 160, http://dx.doi.org/10.1088/0959-5309/57/3/302
20. M. Chaitanya Varma et.al., effect of particle size on saturation magnetization and magnetic anisotropy of Ni0.65Zn0.35Fe2O4 nanoparticles, *International Journal of Nanosci* **2012**,11, 1240003. https://doi.org/10.1142/S0219581X12400030.
21. S.A.MazenN.I.Abu-ElsaadA.E.Khadour, A comparative study of the structural and magnetic properties for Zn^{2+} and Ge^{4+} ions substituted nickel ferrites, Journal of Magnetism and Magnetic Materials 2019,491, 165562, https://doi.org/10.1016/j.jmmm.2019.165562.
22. N. Raghuram, T. Subba Rao, K. Chandra Babu Naidu, Electrical and impedance spectroscopy properties of hydrothermally synthesized $Ba_{0.2}Sr_{0.8-y}La_yFe_{12}O_{19}$ (y = 0.2 - 0.8) nanorods, *Ceramics International* **2020**, 46, 5894-5906, https://doi.org/10.1016/j.ceramint.2019.11.042
23. N. Raghuram, T. S. Rao, K. Chandra Babu Naidu, Investigations on Functional Properties of Hydrothermally Synthesized $Ba_{1-x}Sr_xFe_{12}O_{19}$ (x = 0.0 - 0.8) Nanoparticles, *Material Science in Semiconductor Processing* **2019**, 94, 136-150, https://doi.org/10.1016/j.mssp.2019.01.037.
24. C.Shivakumara, Low-temperature synthesis and characterization of rare earth orthoferrites $LnFeO_3$(Ln=La, Pr and Nd) from molten NaOH flux, *Solid State Communications* **2006**, 139 , 165–169, https://doi.org/10.1016/j.ssc.2006.05.030.
25. M.A.Popov,O.P.Fedorchuk,S.O.Solopan,I.V.Zavislyak,A.G.Belous, Microwave composite structures on the base of nickel-zinc ferrite $Ni_{1-x}Zn_xFe_2O_4$ nanoparticles in the photopolymer matrix, *Journal of Magnetism and Magnetic Materials* **2019**,469,398-404, https://doi.org/10.1016/j.jmmm.**2018**.09.006.
26. O.M. Lemine "Microstructural characterization of α-Fe_2O_3 nanoparticles using, XRD line profiles analysis, FE-SEM and FT-IR", *Superlattices and Microstructures* **2009**, 45, 576-582. https://doi.org/10.1016/j.spmi.**2009**.02.004
27. B.B.V.S.Vara Prasad,K.V.Ramesh, AdirajSrinivas, Physical, structural, morphological, magnetic and electrical properties of $Co_{0.5-x}Ni_xZn_{0.5}Fe_2O_4$ nanocrystalline ferrites, *Ceramic International* 2019, 45, 4549-4563, https://doi.org/10.1016/j.ceramint.2018.11.141.
28. D. Chandra Sekhar, T. Subba Rao, K. Chandra Babu Naidu, Iron deficient $BaNi_xMn_x Fe_{12-2x}O_{19}$ (x=0.0–0.5) hexagonal plates: single-domain magnetic structure and dielectric properties, *Applied Physics A* **2020,** 126,511, https://doi.org/10.1007/s00339-020-03681-5.
29. T. Vidya Sagar, T. Subba Rao, K. Chandra Babu Naidu, Effect of calcination temperature on optical, magnetic and dielectric properties of Sol-Gel synthesized $Ni_{0.2}Mg_{0.8-x}Zn_xFe_2O_4$ (x=0.0–0.8),*Ceramic International* **2020**, 46, 11515-11529, https://doi.org/10.1016/j.ceramint.2020.01.178.
30. Abdul Gafoor, K. Chandra Babu Naidu, D. Ravinder, Khalid Mujasam Batoo, Syed Farooq Adil, Mujeeb Khan, Synthesis of nano-$NiXFe_2O_4$ (X = Mg/Co) by citrate-gel method: structural, morphological and low-temperature magnetic properties, *Applied Physics A* **2020**,126,39 https://doi.org/10.1007/s00339-019-3225-1

31. A.Mallikarjuna, S. Ramesh, N. S. Kumar, K. Chandra Babu Naidu, K. V. Ratnam, H. Manjunatha, B. P. Rao, Structural transformation and high negative dielectric constant behaviour in (1-x) ($Al_{0.2}La_{0.8}TiO_3$) + (x) ($BiFeO_3$) (x = 0.2 - 0.8) nanocomposites, *Physica E: Low-dimensional Systems and Nanostructures* **2020**, 122 ,114204, https://doi.org/10.1016/j.physe.2020.114204.
32. N. Raghuram, T. Subba Rao, K. Chandra Babu Naidu, Magnetic properties of hydrothermally synthesized $Ba_{1-x}Sr_xFe_{12}O_{19}$ (x = 0.0 - 0.8) nanomaterials, *Applied Physics A* **2019**, 125, 839, https:// doi.org/10.1007/s00339-019-3143-2
33. U. Naresh, R. J. Kumar, K. Chandra Babu Naidu, Optical, Magnetic and Ferroelectric Properties of $Ba_{0.2}Cu_{0.8-x}La_xFe_2O_4$ (x = 0.2 - 0.6) Nanoparticles, *Ceramics International* **2019**, 45,7515-7523, https://doi.org/10.1016/j.ceramint.2019.01.044.
34. Nehru Boda, K. Chandra Babu Naidu, D. Baba Basha, D. Ravinder, Structural and Magnetic Properties of $CdCoFe_2O_4$ Nanoparticles, *Journal of Superconductivity and Novel Magnetism* **2019**, 33,1039-1044, https://doi.org/10.1007/s10948-019-05242-1.
35. N. Boda, G. Boda, K. Chandra Babu Naidu, M. Srinivas, K. M. Batoo, D. Ravinder, A.P. Reddy, Effect of Rare Earth Elements on Low Temperature Magnetic Properties of Ni and Co-Ferrite Nanoparticles, *Journal of Magnetism and Magnetic Materials* **2019**, 473, 228-235, https:// doi.org/10.1016/j.jmmm.2018.10.023
36. U. Naresh, R. J. Kumar, K. Chandra Babu Naidu, Hydrothermal synthesis of barium copper ferrite nanoparticles: Nanofiber formation, optical, and magnetic properties, *Materials Chemistry and Physics* **2019**, 236 , 121807, https:// doi.org/10.1016/j.matchemphys.2019.121807
37. Vinuthna C H, K. Chandra Babu Naidu, Chandra Sekhar C, Ravinder D, Magnetic and Antimicrobial Properties of Cobalt Zinc Ferrite Nanoparticles Synthesized By Citrate-Gel Method, *International Journal of Applied Ceramic Technology* **2019**, https://doi.org/10.1111/ijac.13276,
38. G.Luo,W.Zhou,J.Li,Z.Zhou,G.Jiang,W.Li,S.Tang,Y.Du,The influence of Nd^{3+} on doping on structural,dielectric and magnetic properties of Ni–Znferrites,*J.Mater.Sci.Mater.Electron.* **2017**, 28 , 7259–7263. https://doi.org/10.1007/s10854-017-6408-6
39. L.Zhao, H.Yang, L.Yu, Y.Cui, X.Zhao. S.Feng, Magnetic properties of Re-substituted Ni–Mn ferrite nanocrystallites, *J.Mater.Sci*. **2007**, 42, 686-691, https://doi.org/10.1007/s10853-006-0273-7.
40. KunQian,ZhengjunYao,HaiyanLin,JintangZhou,Azhar Ali Haidry, TongbaihuiQi, WenjingChen, XinluGuo, The influence of Nd substitution in Ni–Zn ferrites for the improved microwave absorption properties, *Ceramic International* **2020**, 46 , 227-235, https://doi.org/10.1016/j.ceramint.2019.08.255.
41. Yehia, M., Ismail, S.M. &Hashhash, A. "Structural and Magnetic Studies of Rare-Earth Substituted Nickel Ferrites" *J Supercond Nov Magn* **2014**, 27 ,771-774, https://doi.org/10.1007/s10948-013-2340-z.
42. Dalal,M.;Mallick,A.;Mahapatra,A.S.;Mitra,A.;Das,A.;Das,D.;Chakrabarti,P.K.Effect of cation distribution on the magnetic and hyperfine behaviour of nanocrystalline Co doped NiZnferrite ($Ni_{0.4}Zn_{0.4}Co_{0.2}Fe_2O_4$).*Mater.Res.Bull.***2016**,*76*,389401,https://doi.org/10.1016/j.materresbull.2015.12.028
43. N. Raghuram, T. Subba Rao, N. Suresh Kumar, K. Chandra Babu Naidu, H. Manjunatha, B. Ramakrishna Rao, Anish Khan, Abdullah M. Asiri, $BaSrLaFe_{12}O_{19}$ nanorods: Optical and magnetic properties, *Journal of Materials Science: Materials in Electronics* **2020**, 31,8022-8032, https://doi.org/10.1007/s10854-020-03342-6.
44. K. Chandra Babu Naidu and W. Madhuri, Ceramic nanoparticle synthesis at lower temperatures for LTCC and MMIC technology, *IEEE Transactions on Magnetics* **2018**, 54, 2300808, https:// doi.org/10.1109/TMAG.2018.2855663.